



## Supplementary Information

### Upconversion 3D Printed Composite with Multifunctional Applications for Tissue Engineering and Photodynamic Therapy

*Karina Nigoghossian, \*,<sup>#,a</sup> Sybele Saska,<sup>#,a</sup> Livia M. Christovam,<sup>a</sup> Fernanda Coelho,<sup>b</sup> Cesar Augusto G. Beatrice,<sup>c</sup> Alessandra A. Lucas,<sup>c</sup> Paulo I. Neto,<sup>d</sup> Jorge Vicente L. da Silva,<sup>d</sup> Agnieszka Tercjak, <sup>e</sup> Maurício S. Baptista,<sup>f</sup> Luiz Henrique Catalani,<sup>f</sup> Raquel M. Scarel-Caminaga,<sup>b</sup> Ticiano S. O. Capote<sup>b</sup> and Sidney José L. Ribeiro<sup>\*,a</sup>*

<sup>a</sup>*Instituto de Química, Universidade Estadual Paulista (Unesp), 14800-900 Araraquara-SP, Brazil*

<sup>b</sup>*Faculdade de Odontologia, Universidade Estadual Paulista (Unesp), 14801-903 Araraquara-SP, Brazil*

<sup>c</sup>*Departamento de Engenharia de Materiais, Universidade Federal de São Carlos (UFSCar), 13565-905 São Carlos-SP, Brazil*

<sup>d</sup>*Núcleo de Tecnologias Tridimensionais, Centro de Tecnologia da Informação Renato Archer (CTI), 13069-901 Campinas-SP, Brazil*

<sup>e</sup>*Group “Materials + Technologies” (GMT), Department of Chemical and Environmental Engineering, Engineering College of Gipuzkoa, University of the Basque Country (UPV/EHU), 20018 Donostia-San Sebastián, Spain*

<sup>f</sup>*Instituto de Química, Universidade de São Paulo (USP), 05508-000 São Paulo-SP, Brazil*

---

\*e-mail: karina.nig@gmail.com; sidney.jl.ribeiro@unesp.br

<sup>#</sup>The authors contributed equally to this work.

## Experimental details

X-rays diffraction profiles (XRD) measurements were performed on a Siemens Kristalloflex diffractometer using nickel-filtered and  $\text{CuK}\alpha$  radiation. The operation voltage and current were kept at 40 kV and 40 mA, respectively, between angles of  $15^\circ$  to  $90^\circ$  in steps of  $0.01^\circ$  with a 10-s count time. Scanning electron microscopy (SEM) was used for the morphological analysis. Morphology of UCNP s was examined by SEM using a LEO 440 equipment equipped with an OXFORD detector. The micrographs of UCNP s-apatite and PCL/UCNP s-apatite were obtained in a FEI electronic microscope, model Magellan 400L, equipped with an EDAX brand Apollo X detector. The samples were covered by a gold layer of thickness of 6 nm (20 s, voltage of 3 kV and current of 15 mA). The computer software ImageJ<sup>1</sup> was used to analyze the SEM image of PCL/UCNP s-apatite.

## Characterizations of materials

Figure S1A shows a photograph of the PCL/UCNP s-apatite filament extruded in a twin-screw extruder with a diameter of 1.8 mm. From such filament, the scaffolds were obtained using additive manufacturing (3D printing) with dimensions  $20 \times 20 \times 2$  mm (length  $\times$  width  $\times$  height) and 500  $\mu\text{m}$  pores. The photograph of the PCL/UCNP s-apatite scaffold is shown in Figure S1B.

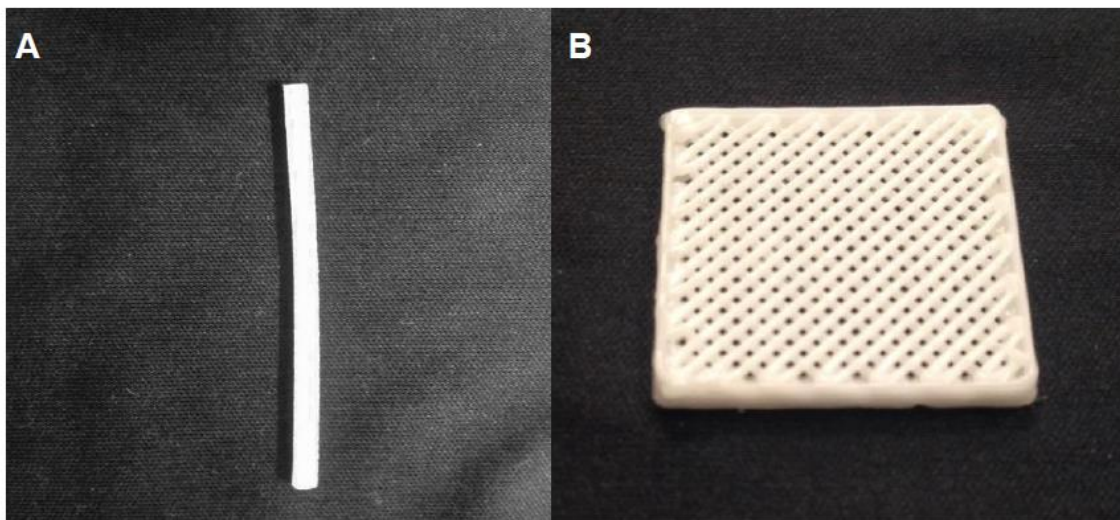


**Figure S1.** Photograph of the PCL/UCNP s-apatite filament (A) and scaffold (B).

Figure S2A displays a typical SEM image of UCNP s. Particles with sizes below 100 nm can be observed together with larger agglomerates of particles. SEM image of UCNP s-apatite is shown in Figure S2B. The scaling structure observed demonstrates that the material does not have a defined shape. Figure S2C shows SEM cross-section image of the PCL/UCNP s-apatite filament. The homogeneous distribution of UCNP s-apatite throughout the extension of the material is evidenced by the contrast between the dark PCL host and the grey UCNP s-apatite particles. Average Feret diameter of UCNP s-apatite particles is  $3.38 \pm 0.95 \mu\text{m}$  ( $n = 100$ ). The distribution (D) of UCNP s-apatite *per* area (A) was calculated by the following equation:

$$D (\%) = [A_{\text{UCNPs-apatite}} / A_{\text{total}} - A_{\text{UCNPs-apatite}}] \times 100 \quad (\text{S1})$$

UCNPs-apatite makes 4.42% of all area of the PCL/UCNPs-apatite filament.

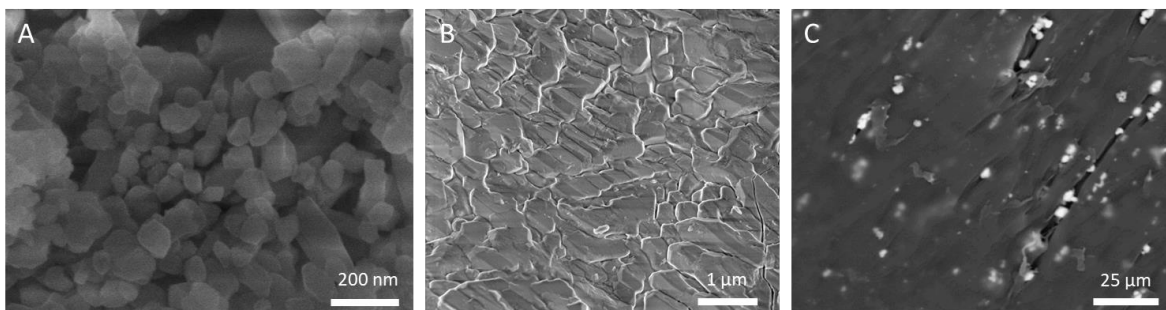
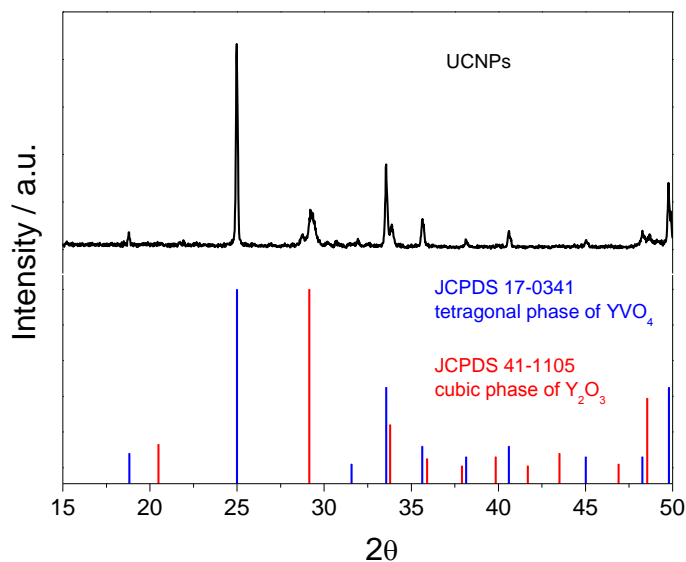


**Figure S2.** SEM image of UCNPs (A), UCNPs-apatite (B) and PCL/UCNPs-apatite (C).

Figure S3 shows the X-ray diffraction (XRD) pattern and phase references for UCNPs. The main reflections in the diffraction pattern are related to the tetragonal phase of  $\text{YVO}_4$  (JCPDS Card No. 17-0341). The  $\text{Y}_2\text{O}_3$  cubic phase (JCPDS Card No. 41-1105) is also observed. The crystallite size was estimated using Scherrer's equation:<sup>2</sup>

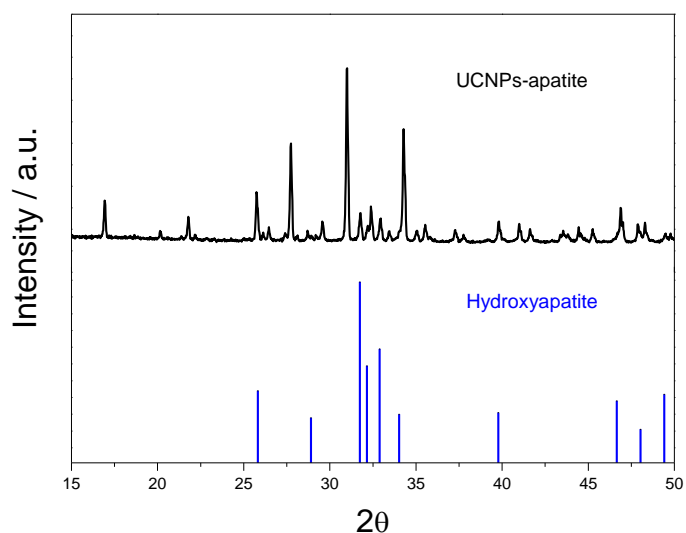
$$D_{\text{hkl}} = 0.89 \frac{\lambda}{(B \cos \theta)} \quad (\text{S2})$$

In this equation, the crystallite domain size is calculated from the width of the diffraction peak (B),  $\lambda$  is the wavelength of  $\text{CuK}\alpha$  radiation (0.15418 nm), and  $\theta$  is angle of the corresponding diffraction peak. A crystallite size value of approximately 78 nm was obtained for the full width at the half-maximum of the diffraction peak (200) at  $25^\circ$ .



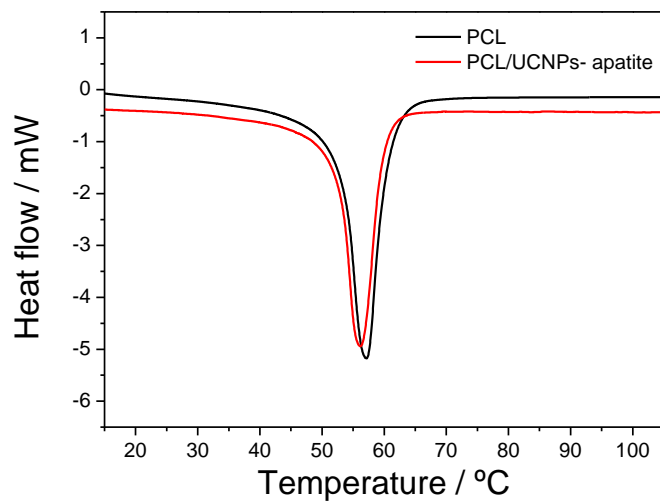
**Figure S3.** XRD pattern of UCNPs. Reference diffraction peaks corresponds to tetragonal phase of  $\text{YVO}_4$  (JCPDS Card No. 17-0341) and  $\text{Y}_2\text{O}_3$  cubic phase (JCPDS Card No. 41-1105).

Figure S4 shows the XRD pattern of UCNPs-apatite and phase reference for hydroxyapatite. The main diffraction peaks correspond to hydroxyapatite standard but shifted to lower  $2\theta$  values. This effect may be caused by the replacement of phosphorus by vanadium atoms in the crystalline matrix. The shifted diffraction peaks are related to the size difference between phosphorus and vanadium atoms. The absence of crystal phase related to  $YVO_4$  suggests the incorporation of UCNPs into the hydroxyapatite crystal lattice. Batista *et al.*<sup>3</sup> investigated the crystalline structure of phosphovanadates.  $YPO_4$  and  $YVO_4$  have the same tetragonal structure, however the larger ionic volume of the  $VO_4^{3-}$  groups as compared to that of  $PO_4^{3-}$  makes the diffraction peaks shift to lower angle values when vanadium concentrations increased.



**Figure S4.** XRD pattern of UCNPs-apatite. Reference diffraction peaks corresponds to hydroxyapatite.<sup>4</sup>

Figure S5 shows DSC heating scans for PCL and PCL/UCNPs-apatite.



**Figure S5.** DSC curves for PCL and PCL/UCNPs-apatite.

## References

1. Rasband, W. S.; *ImageJ*, version 1.52a; U. S. National Institutes of Health, Bethesda, Maryland, USA, 2011.
2. Langford, J. I.; Wilson, A. J. C.; *J. Appl. Crystallogr.* **1978**, *11*, 102.
3. Batista, J. C.; de Sousa Filho, P. C.; Serra, O. A.; *Dalton Trans.* **2012**, *41*, 6310.
4. Hattori, T.; Lwadata, Y.; *J. Am. Ceram. Soc.* **1990**, *71*, 1803.

